Technical Document 1544
May 1989

Demonstration of a Dual-Lidar Method for Measuring Optical Depths in the Vertical

Merle R. Paulson
Douglas R. Jensen

NAVAL OCEAN SYSTEMS CENTER

San Diego, California 92152-5000

E. G. SCHWEIZER, CAPT, USN
Commander

R. M. HILLYER
Technical Director

ADMINISTRATIVE INFORMATION

The work reported herein was conducted for the Office of Naval Technology over the period October 1988 to May 1989.

Released by
H. V. Hitney,
Tropospheric Branch

Under authority of
J. H. Richter, Head
Ocean and Atmospheric
Sciences Division

AS

REPORT DOCUMENTATION PAGE

1a. REPORT SECURITY CLASSIFICATION UNCLASSIFIED	1b. RESTRICTIVE MARKINGS
2a. SECURITY CLASSIFICATION AUTHORITY	3. DISTRIBUTION/AVAILABILITY OF REPORT Approved for public release; distribution is unlimited.
2b. DECLASSIFICATION/DOWNGRADING SCHEDULE	
4. PERFORMING ORGANIZATION REPORT NUMBER(S) NOSC TD 1544	5. MONITORING ORGANIZATION REPORT NUMBER(S)
6a. NAME OF PERFORMING ORGANIZATION Naval Ocean Systems Center 6b. OFFICE SYMBOL (If applicable) NOSC	7a. NAME OF MONITORING ORGANIZATION
6c. ADDRESS (City, State and ZIP Code) San Diego, California 92152–5000	7b. ADDRESS (City, State and ZIP Code)
8a. NAME OF FUNDING/SPONSORING ORGANIZATION Office of Naval Technology 8b. OFFICE SYMBOL (If applicable) Code 228	9. PROCUREMENT INSTRUMENT IDENTIFICATION NUMBER
8c. ADDRESS (City, State and ZIP Code) 800 N. Quincy St. Arlington, VA 22217-5000	10. SOURCE OF FUNDING NUMBERS PROGRAM ELEMENT NO.: 0602435N PROJECT NO.: RM35G80 TASK NO.: AGENCY ACCESSION NO.: DN488 760

11. TITLE (Include Security Classification)

DEMONSTRATION OF A DUAL-LIDAR METHOD FOR MEASURING OPTICAL DEPTHS IN THE VERTICAL

12. PERSONAL AUTHOR(S)

M. R. Paulson, D. R. Jensen

13a. TYPE OF REPORT	13b. TIME COVERED	14. DATE OF REPORT (Year, Month, Day)	15. PAGE COUNT
Final	FROM Oct 1988 TO May 1989	May 1989	32

16. SUPPLEMENTARY NOTATION

17. COSATI CODES			18. SUBJECT TERMS (Continue on reverse if necessary and identify by block number)
FIELD	GROUP	SUB-GROUP	atmospheric aerosols optical backscatter extinction coefficient

19. ABSTRACT (Continue on reverse if necessary and identify by block number)

Experimental results are reported of optical depth measurements in the vertical direction. A dual-lidar method for measuring extinction coefficient profiles was employed. The mathematical derivations of the method are described.

20. DISTRIBUTION/AVAILABILITY OF ABSTRACT	21. ABSTRACT SECURITY CLASSIFICATION	
☐ UNCLASSIFIED/UNLIMITED ☒ SAME AS RPT ☐ DTIC USERS	UNCLASSIFIED	
22a. NAME OF RESPONSIBLE INDIVIDUAL M. R. Paulson	22b. TELEPHONE (Include Area Code) (619) 553–1413	22c. OFFICE SYMBOL Code 543

DD FORM 1473, 84 JAN

83 APR EDITION MAY BE USED UNTIL EXHAUSTED
ALL OTHER EDITIONS ARE OBSOLETE

UNCLASSIFIED

SECURITY CLASSIFICATION OF THIS PAGE (When Data Entered)

DD FORM 1473, 84 JAN

UNCLASSIFIED

SECURITY CLASSIFICATION OF THIS PAGE (When Data Entered)

CONTENTS

ILLUSTRATIONS

ILLUSTRATIONS (continued)

INTRODUCTION

Lidar has become a very popular instrument for use in the study of atmospheric extinction. Lidar theory, however, suffers from the limitation that, while there is only one equation, there are two unknowns. Most people using lidars avoid this problem by making assumptions about the relationship between these unknowns, or make assumptions about the characteristics of the atmospheric aerosols.

One assumption that is sometimes made is that the atmosphere is horizontally homogeneous. A more frequently used assumption is that the relationship between backscatter and extinction is a constant. These assumptions are often not justified.

Paulson (1986) reports that lidar returns frequently show pronounced horizontal atmospheric inhomogeneities. Figure 1 shows two examples of this. The curves are the natural logarithm of the range-compensated power received plotted as a function of range. If the atmosphere were homogeneous along the propagation path, these curves would be straight lines, with the magnitude of the slope equal to twice the atmospheric extinction coefficient.

Workers who assume constant backscatter-to-extinction ratios usually make a guess as to what this ratio is and proceed from there. Fenn (1966), however, states that theoretical considerations show that no generally valid relation exists between the atmospheric extinction coefficient and the atmospheric backscatter properties. He further says that it is therefore clear that such a relation cannot be unique and will change from one situation to another.

Mulders (1984) states that the relationship between backscatter and extinction may be very sensitive to the chemical composition of the aerosol. His measurements, he says, show that it may vary during one day in one place. When data for one month were considered, no relationship between backscatter coefficient and extinction coefficient was evident.

A dual-lidar method for measuring extinction coefficient profiles was proposed by Paulson and Powers in late 1985. This method uses two lidars set at opposite ends of a propagation path and pointed at each other. No assumptions need to be made about the atmosphere since there are now two equations available, and the extinction coefficient profile, integrated extinction, and the backscatter coefficient profile can be obtained. The theory is discussed in detail by Paulson (1987) and by Hughes and Paulson (1988).

Recently, Kunz (1987) has suggested the same technique with a somewhat different mathematical approach, but it appears that he has not tested it yet.

The purpose of this report is to describe and demonstrate an extension of this technique to obtain optical depth measurements in the vertical direction. While the mathematical derivations have been documented in previous reports, they are repeated here for completeness.

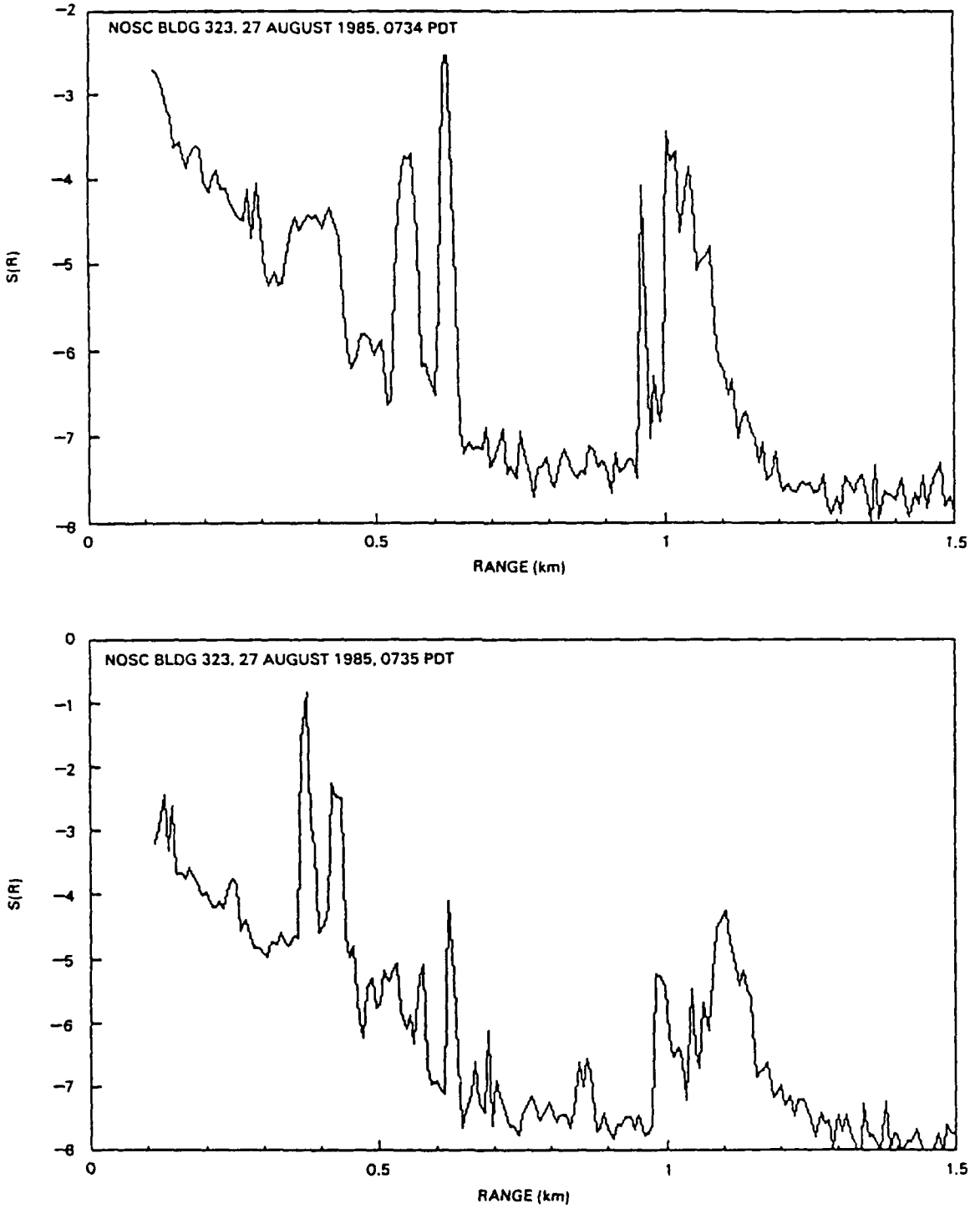

Figure 1. *S(R)* data plotted as a function of range for lidar #025091 taken on 27 August 1985. Visibility was about 10 km.

MATHEMATICAL DERIVATIONS

EXTINCTION COEFFICIENT PROFILES

The quantity $S(R)$ is the natural logarithm of the backscattered power received from range R, multiplied by R^2. If the two lidars are separated a distance d, as shown in figure 2, and the origin is at lidar l, the equation for $S(R)$ for the first lidar is

$$S_1(R) = ln(C_{11}) + ln[\beta(R)] - \int_0^R \sigma(r)dr \tag{1}$$

and that for the second lidar is

$$S_2(R) = ln(C_{12}) + ln[\beta(R)] - 2\int_R^d \sigma(r)dr \tag{2}$$

where C_{11} and C_{12} are the instrumentation constants for each of the lidars, $\sigma(r)$ is the extinction coefficient at range r, and $\beta(R)$ is the backscatter coefficient at range R.

If equation (2) is subtracted from equation (1) we get

$$S_1(R) - S_2(R) = ln(C_{11} - ln(C_{12}) - 2\int_0^R \sigma(r)dr + 2\int_R^d \sigma(r)dr\ . \tag{3}$$

Since

$$\int_R^d \sigma(r)dr = \int_0^d \sigma(r)dr - \int_0^R \sigma(r)dr\ , \tag{4}$$

equation (3) becomes

$$S_1(R) - S_2(R) = ln(C_{11} - ln(C_{12}) - 4\int_0^R \sigma(r)dr + 2\int_0^d \sigma(r)dr\ . \tag{5}$$

Taking the difference between equations (1) and (2) eliminates the backscatter coefficient. Taking the derivative of equation (5) eliminates the requirement that constants C_{11} and C_{12} be known, and we get

$$dS_1(R) - dS_2(R) = -4\sigma(R)dR \tag{6}$$

or

$$\sigma(R) = \frac{\frac{dS_2(R)}{dR} - \frac{dS_1(R)}{dR}}{4}\ . \tag{7}$$

The calibration curves for each of the lidar receivers are still needed, however, and must be accurately known since they affect the slope characteristics of the $S(R)$ curves. Since the propagation for the two lidars is in opposite directions with respect to the origin, the slopes of $S_1(R)$ and $S_2(R)$ should have opposite signs under homogeneous conditions.

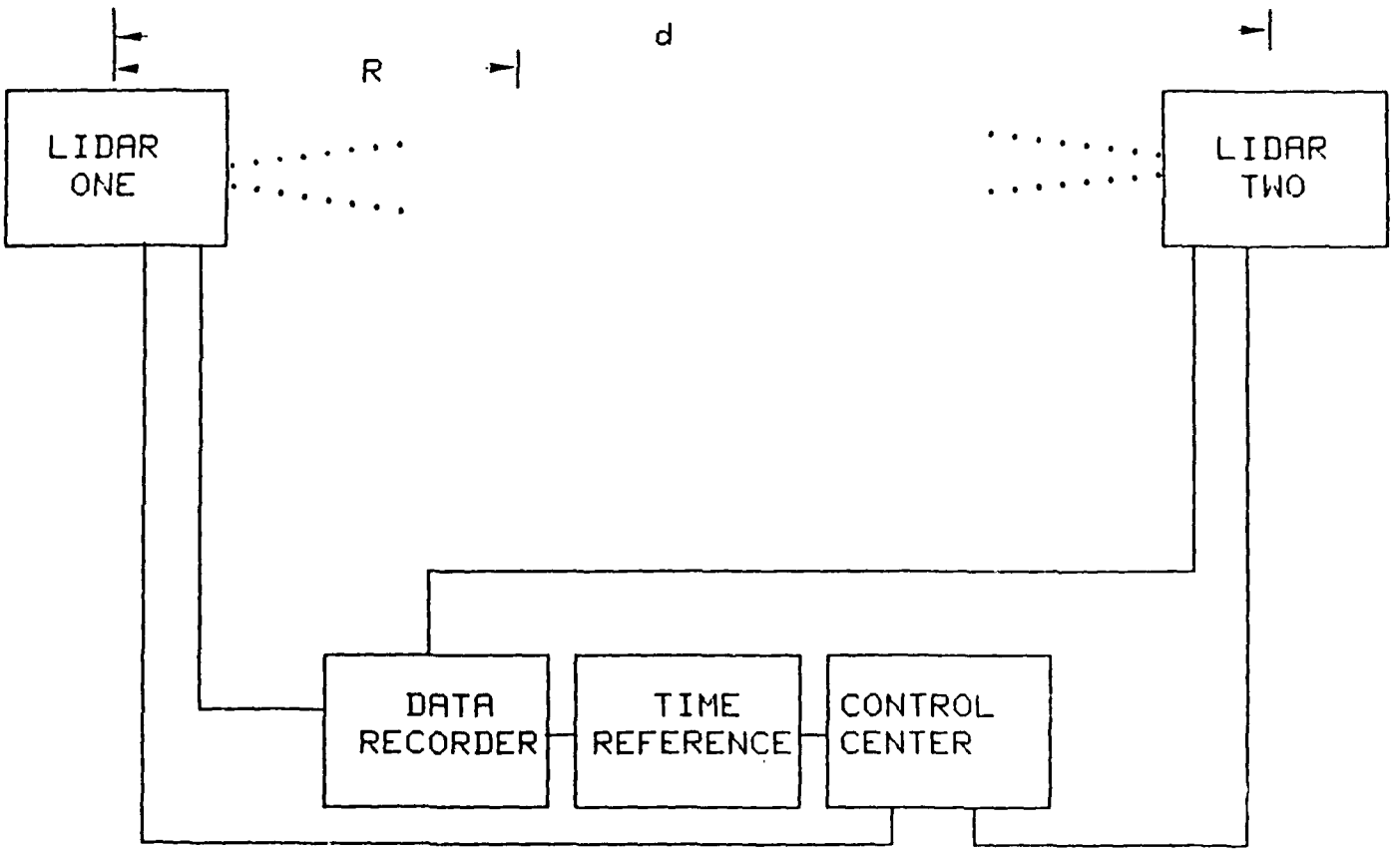

Figure 2. Block diagram of a possible dual-lidar system for measuring atmospheric extinction and backscatter coefficient profiles.

INTEGRATED EXTINCTION OR OPTICAL DEPTH

While equation (7) will give good extinction-coefficient profiles under many conditions, small-scale irregularities in the atmospheric aerosols may be seen somewhat differently by the two lidars. This can cause brief positive excursions in the *S(R)* difference curve, which can appear as negative extinction coefficients. In a ground-based system this condition can be minimized by careful alignment of the two lidars so that they are looking along exactly the same path; but in the case of a vertical system, where one lidar is in an aircraft, this is not so easy. It appears, however, that the integrated extinction, or optical depth, obtained from the *S(R)* difference curve is not so sensitive to these positive excursions.

If equation (7) is integrated between two distances, R_1 and R_2, we get

$$\int_{R_1}^{R_2} \sigma(r)dr = \frac{[S_1(R_1) - S_2(R_1)] - [S_1(R_2) - S_2(R_2)]}{4} \quad . \tag{8}$$

Therefore, just taking the difference in the *S(R)* difference curve at Range(1) and Range(2) and dividing by 4 gives the integrated extinction over that distance.

LIDAR CALIBRATION

The lidars used in these measurements were Visioceilometer lidars operating at 1.06 μm wavelength.

Lidar 2 (#025091) was calibrated with the assistance of personnel at TNO in the Netherlands (Ferguson & Paulson, 1986). It was subsequently recalibrated along with lidar 1 (#025090) using neutral density filters. Neutral density filters from 0 to 70 dB in 5-dB steps were placed in front of the lidar receiver. Several shots were made at each attenuation and these were averaged. A fifth-order fit was made for the recorded signal amplitude versus the attenuation for each of the lidars.

LIDAR COMPARISON

The two lidars were set up side by side overlooking the ocean at an elevation of about 30 m. Elevation angle for each was adjusted so that the cross hair rested on the horizon. The vertical cross hair for each lidar was aligned on the mast of a sailboat about 4 or 5 miles away to make sure that they were aligned in azimuth. The two lidars were then fired nearly simultaneously for a number of shots. Figure 3 shows a comparison of the S(R) curves for two of these shots. These show quite good agreement out to about 1 km. Background noise becomes important beyond that.

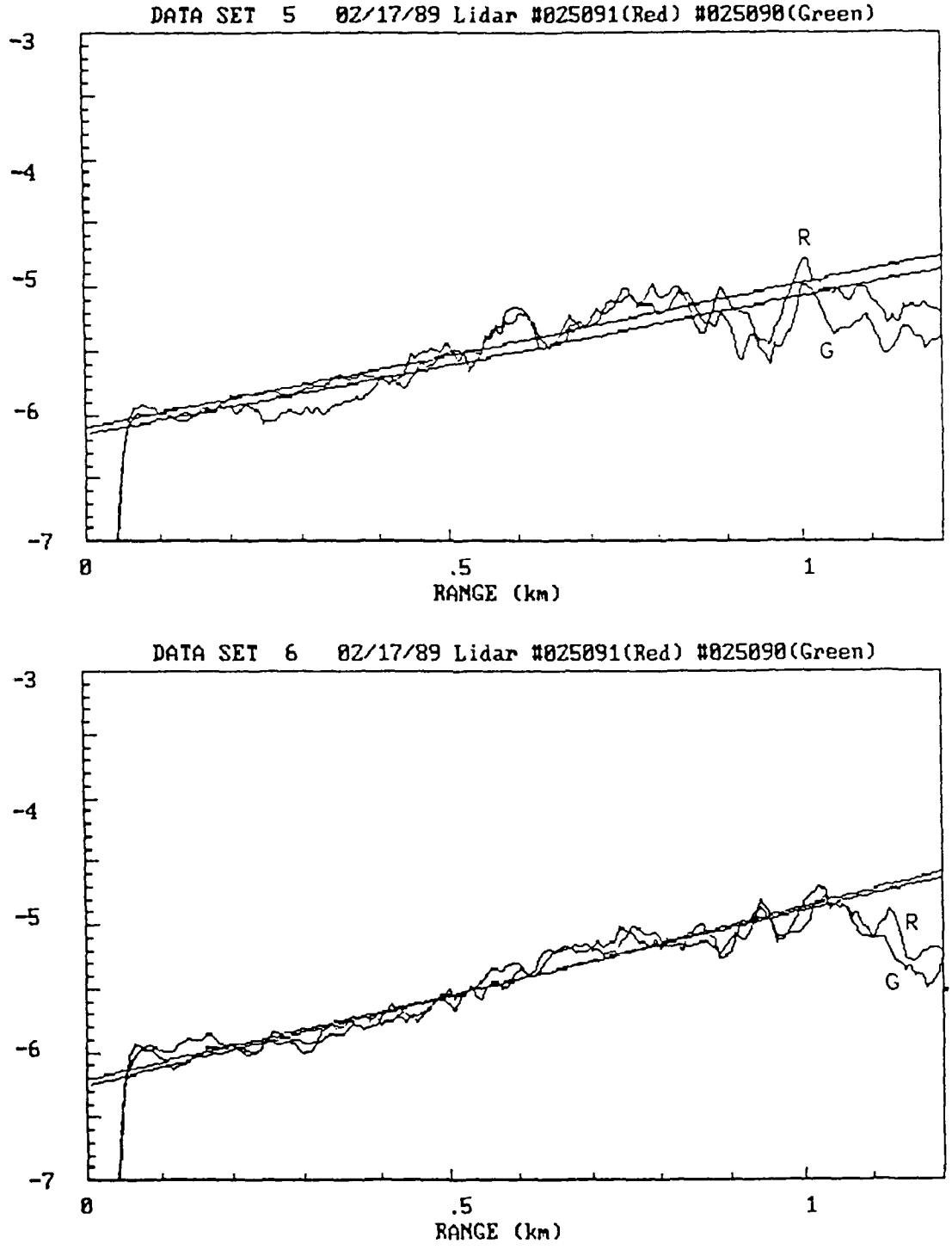

Figure 3. Comparison of the two lidars fired along a parallel horizontal path over the ocean. The increasing *S(R)* with range would indicate a gradient in the aerosol distribution.

VERTICAL MEASUREMENTS

EQUIPMENT SETUP

The first lidar was mounted on a tripod and pointed in the vertical direction. The location of this lidar was at NOSC building 15 at the south end of Point Loma. This site was about 25 to 30 m above sea level. The second lidar was installed in a Piper Navajo aircraft and pointed vertically down through a hole in the floor.

The aircraft made repeated passes over the ground site at a constant altitude of 2500 ft, or about 760 m above the ground site. Personnel on the ground directed the aircraft via radio and, when it was directly over the ground site, called "mark," and both lidars were fired. The data were recorded on Memodyne digital tape recorders for later processing.

DATA ANALYSIS AND RESULTS

The first set of data was taken on 30 March 1989. Ten passes were made at about 3- or 4-min intervals, resulting in eight data samples. The lidar in the aircraft failed to fire the first two passes.

The upper graph in figure 4 shows an example of the range-compensated returns for the two lidars. The lower graph shows the same thing, but with a seven-point running average. Minimum altitude for the ground lidar was about 100 m. This is the point where the laser beam and the receiver field-of-view overlap. The near point for the aircraft lidar was about 680 m, or about 90 m below the aircraft.

Figure 5 shows the same thing for the following pass, Data Set 4. In this case atmospheric conditions at the ground changed in such a way that the digitizer limited for return signals closer than about 120 m. (This point is marked with an arrow in the upper graph.) This also had the effect of reducing signal strength from higher altitudes so that signal returned from greater than 450 m altitude was in the background noise. This same limiting occurred for Data Sets 5 and 6.

S(R) difference curves are shown in figure 6 for the seven-point running averages for these two data sets. Theoretically the slope of these curves should never go positive, which would imply negative extinction. While the slope for Data Set 3 is generally negative, there are some positive perturbations on it. These are the result of very small irregularities, which are seen by the two lidars somewhat differently. Averaging reduces this effect somewhat, but cannot completely eliminate it. In the *S(R)* difference curve for Data Set 4, the curve goes horizontal at about 450 m and then starts to increase. This is the point where the ground lidar return goes into the noise. Below about 120 m the digitizer limited for the ground lidar, otherwise the difference curve might have been somewhat higher in this region.

If we apply equation (8) to the *S(R)* difference curve for Data Set 3, we get an optical depth of 0.20 between the altitudes of 120 and 690 m. Doing the same thing for Data Set 4, we get an optical depth of 0.44 between 130 and 460 m. This has been done for Data Sets 5 through 9 as well and the results shown in table 1. Graphs of these data are in the appendix.

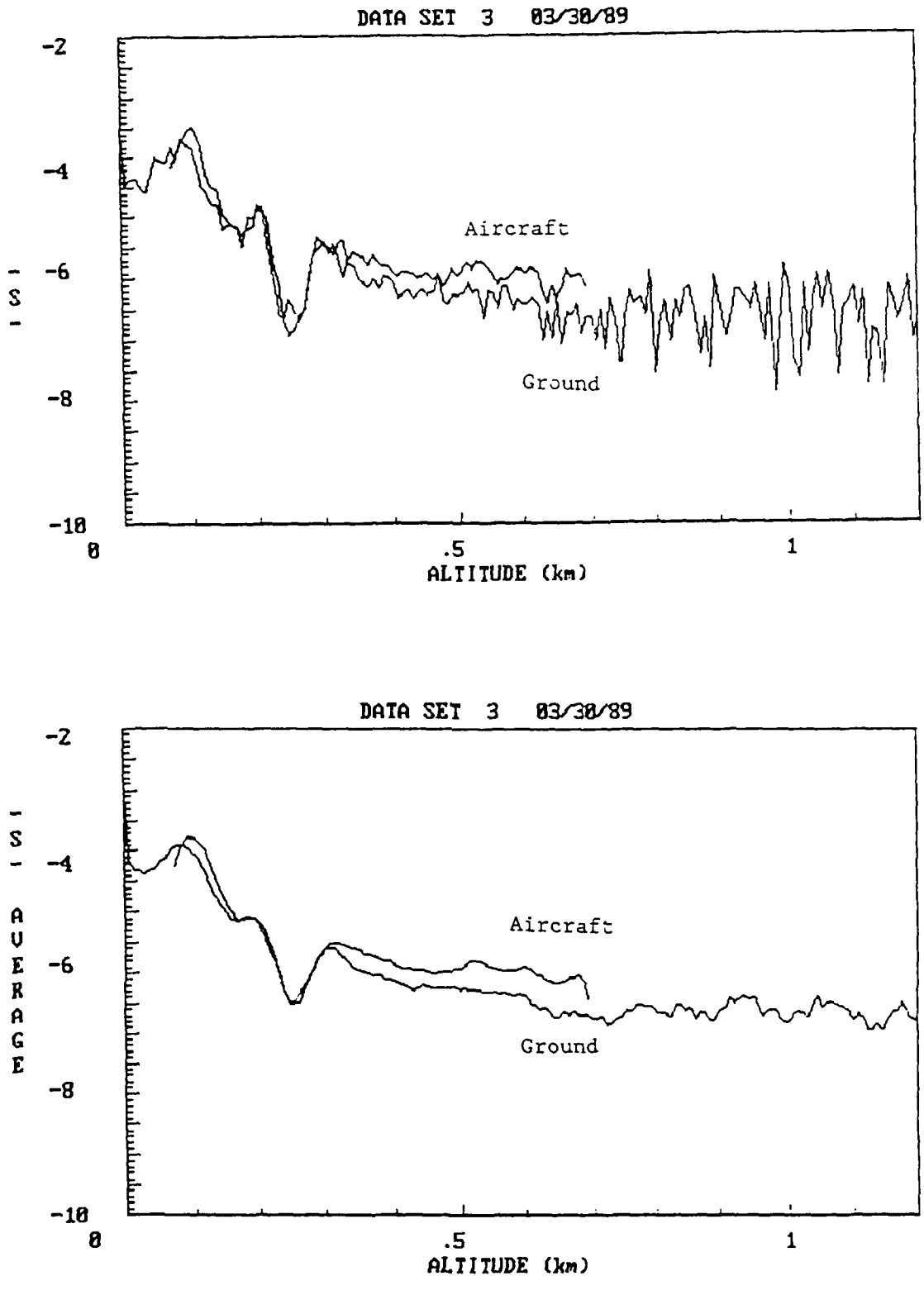

Figure 4. Upper graph is range-compensated lidar returns as a function of altitude for the two lidars for Data Set 3. Lower graph is seven-point running averages for the data shown in the upper graph.

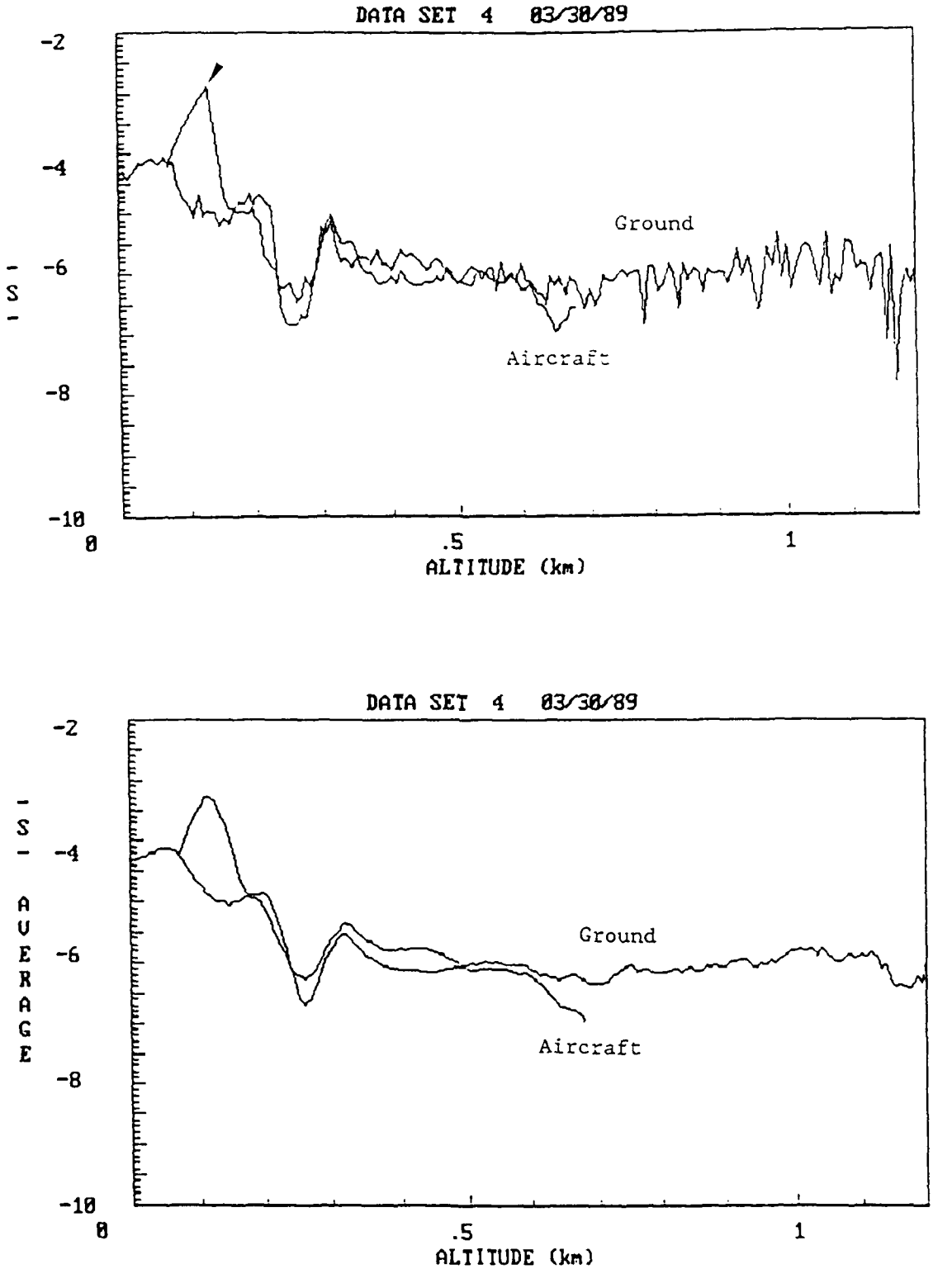

Figure 5. Upper graph is range-compensated lidar returns as a function of altitude for the two lidars for Data Set 4. The arrow shows the altitude below which the digitizer limited. Lower graph is seven- point running averages for the data shown in the upper graph.

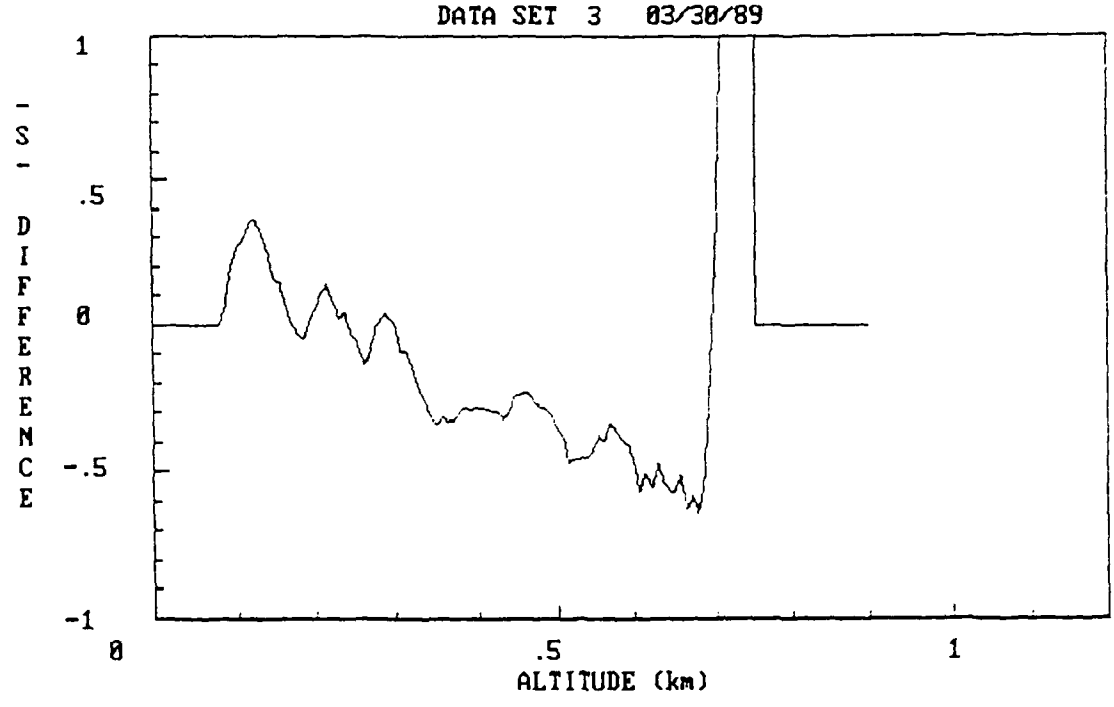

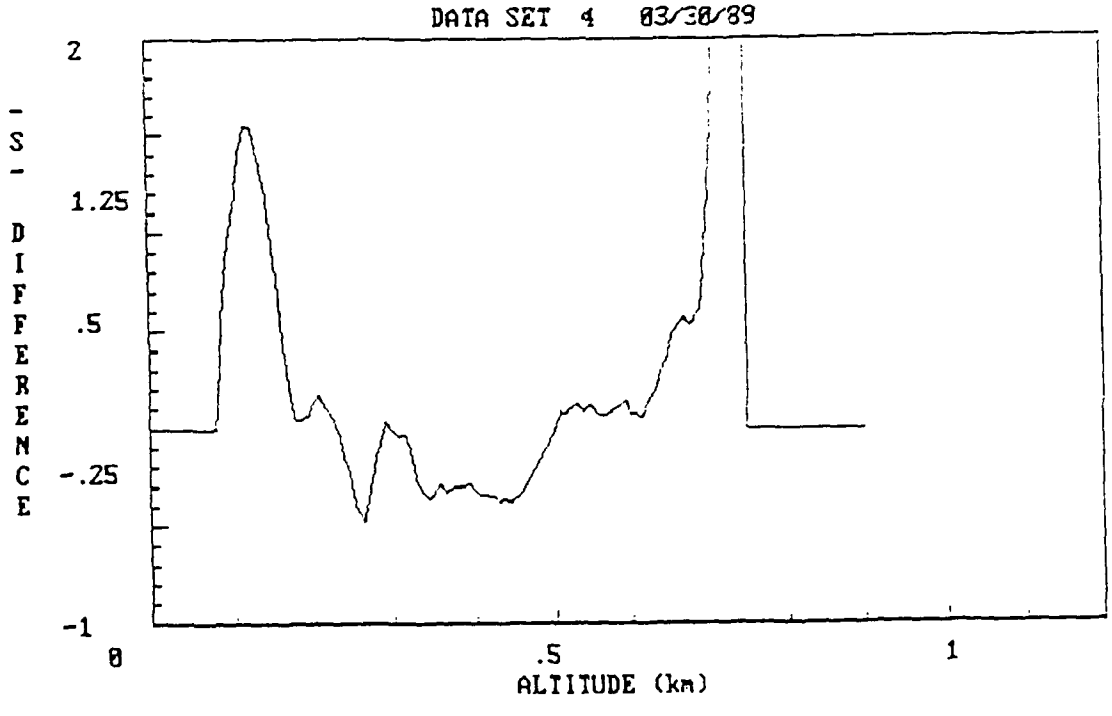

Figure 6. *S(R)* difference curves for Data Sets 3 and 4. In the case of Data Set 4, return from the ground-based lidar goes into the noise at about 450 m altitude.

Table 1. Integrated extinction between the altitudes indicated for each of the data sets. Outside of these altitudes the signal of one of the lidars was either in the noise or the digitizer clipped.

DATA SET	ALTITUDE(m) to	ALTITUDE(m)	OPTICAL DEPTH
3	120	690	0.20
4	130	460	0.44
5	135	590	0.30
6	180	465	0.26
7	160	520	0.16
8	160	460	0.32
9	160	550	0.38

In Data Sets 5 and 9 the return from the airborne lidar dipped down to the noise level near 300 m altitude. This caused a large positive excursion in the *S(R)* difference curve at that point. This probably does not affect the value of the optical depths calculated since the signal is above the noise at the points used for the calculation.

DISCUSSION OF RESULTS

The lidars used have about a 70-dB dynamic range. While this appears to be quite large, variations in atmospheric conditions can greatly exceed it, especially when making measurements in the vertical. In the case of the ground-based lidar, high concentrations of aerosols close to the ground cause strong signal return from close to the lidar, sometimes exceeding the limits of the digitizer. These same high concentrations tend to reduce signal returned from higher up, where there are fewer aerosols and the backscattered signal is weaker. This condition works in favor of the airborne lidar. Since the aircraft is at altitudes where the aerosol concentrations are low, returns from these aerosols are close to the lidar, and the signal-to-noise ratio is good. At lower altitudes, farther from the lidar, the aerosol concentration increases, causing an increase in the strength of the backscattered signal and thus maintaining a good signal-to-noise ratio in most cases. The reverse may also occur when there are stratus conditions. Then the airborne lidar is in, or near, high aerosol concentrations and the one on the ground may not be.

AIRCRAFT CLIMBING SPIRAL TESTS

On completion of the dual-lidar measurements, the aircraft was flown to a location near the Coronodo Islands. There a climbing spiral was made from 100 to 5000 ft while instruments measured dew point, temperature, and aerosol size distributions. At 1000-ft intervals the aircraft leveled momentarily, and the lidar was fired vertically downward.

LIDAR *S(R)* VERSUS RELATIVE HUMIDITY

The lidar shots were combined to generate an *S(R)* profile as a function of altitude up to the 5000-ft level. This curve is shown in figure 7. Dew point and temperature were used to calculate relative humidity as a function of altitude, and it and the *S(R)* profile were compared. This comparison is shown in figure 8. The two curves follow each other quite well from the surface up to about 380 m. Above this altitude the relative humidity remains fairly constant at around 20 percent, but the *S(R)* goes to a minimum of –8.1 then increases again to –6.2 before gradually decreasing again. There does appear to be a tendency for the two curves to follow each other up to at least 800 meters, however. There also is the possibility of aerosols at these altitudes which are not affected by relative humidity.

LIDAR *S(R)* VERSUS KNOLLENBERG *S(R)*

Aerosol sizes were measured continuously from 100 to 5000 ft using a Knollenberg Instrument. These measurements were taken in 4-s sample intervals, and size distributions were calculated for each. A Mie program was used to calculate backscatter and extinction coefficients for each of these samples. The resulting backscatter and extinction coefficients were then used in a lidar equation to calculate an *S(R)* curve as a function of altitude. This curve is shown in figure 9 and compared to that measured with the lidar. The two curves show very good agreement up through the inversion. Above that, the lidar *S(R)*'s are somewhat higher than those calculated from the Knollenberg measurements. Also, the Knollenberg values appear to fluctuate much more. This is because the Knollenberg counts very few aerosols in a sampling period at these altitudes, so the measured distribution is probably not a good indication of the true size distribution for these conditions.

CONCLUSIONS

Under some conditions the dual-lidar method can be used to get measured optical depths in the vertical without making assumptions about the characteristics of the atmospheric aerosol distributions. For this to be done successfully, both lidars must have good signal-to-noise ratios over the height range of interest. At the same time the return signal cannot be so strong as to limit, or have the digitizer clip, at least in the range of interest. Also, some data smoothing is required to reduce the effects of small irregularities, which may be seen somewhat differently by the two lidars.

Range-compensated lidar returns and relative humidity variations showed the same trends up through the inversion. Even above the inversion there was some correspondence. However, it appears that there may be other aerosols contributing to the lidar return in this region that are not dependent on relative humidity.

The range-compensated lidar returns showed good agreement with an *S(R)* curve calculated with the use of Knollenberg aerosol size distributions up through the inversion. It appears, however, that above the inversion the number of aerosols intercepted by the Knollenberg was not sufficient to provide a good measure of the true size distributions.

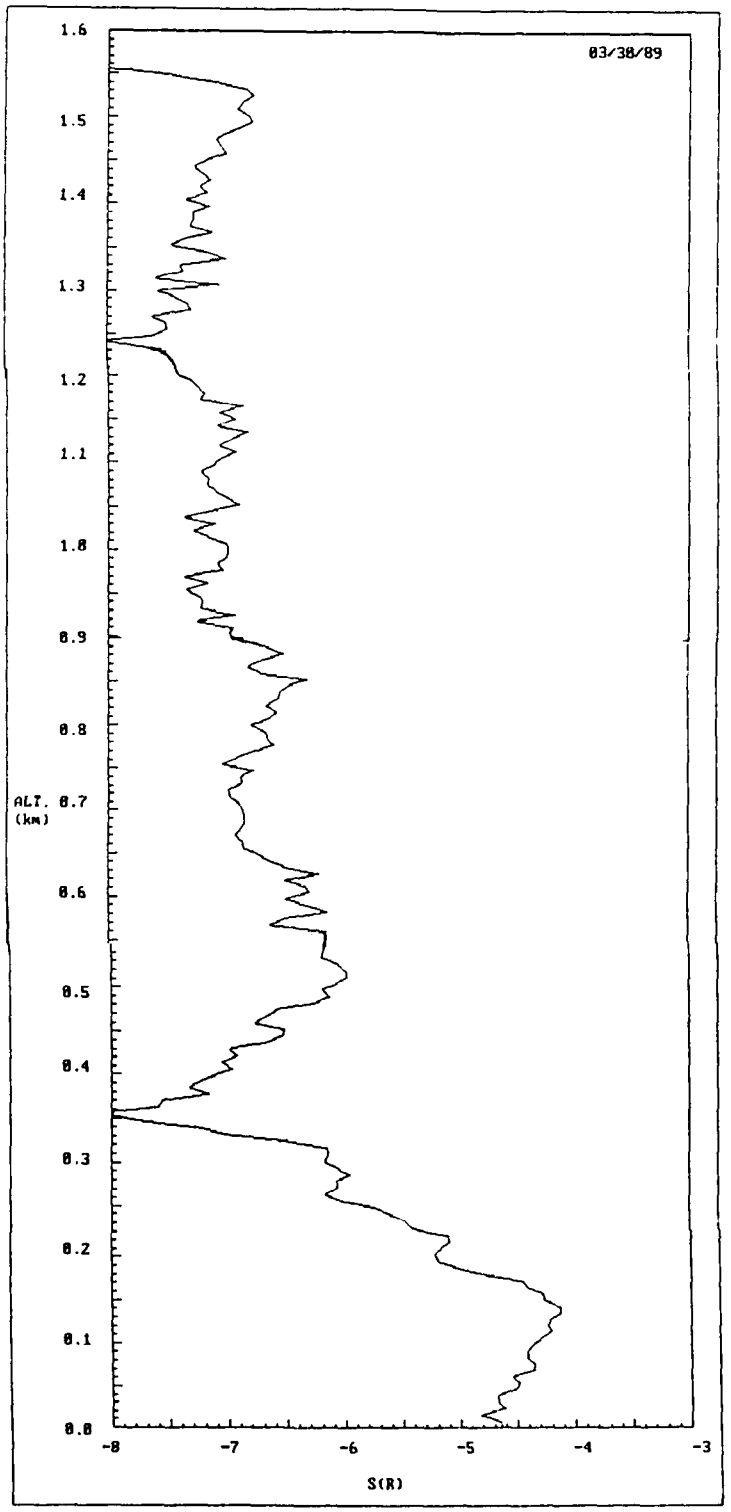

Figure 7. Range-corrected lidar return as a function of altitude.

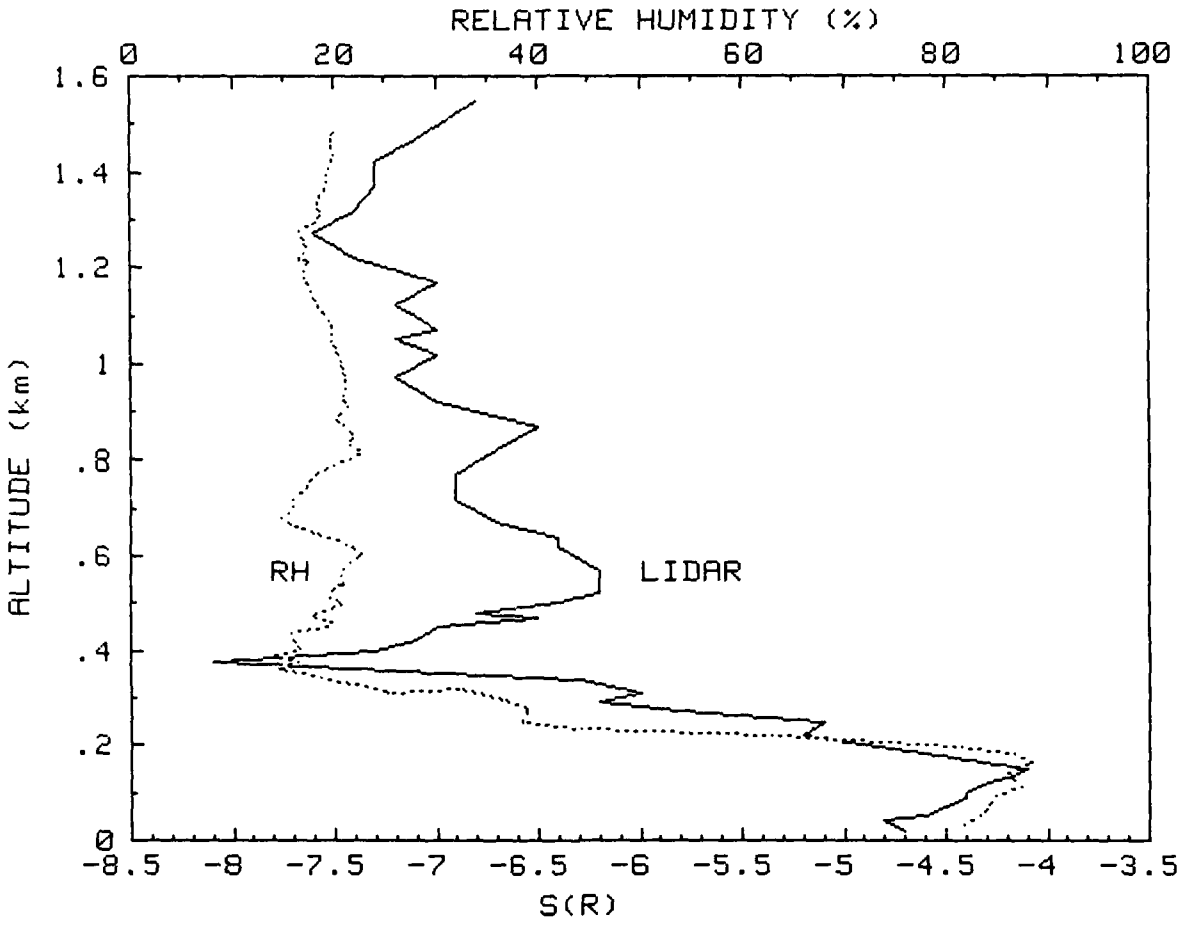

Figure 8. Comparison of range-compensated lidar return as a function of altitude with relative humidity plotted as a function of altitude.

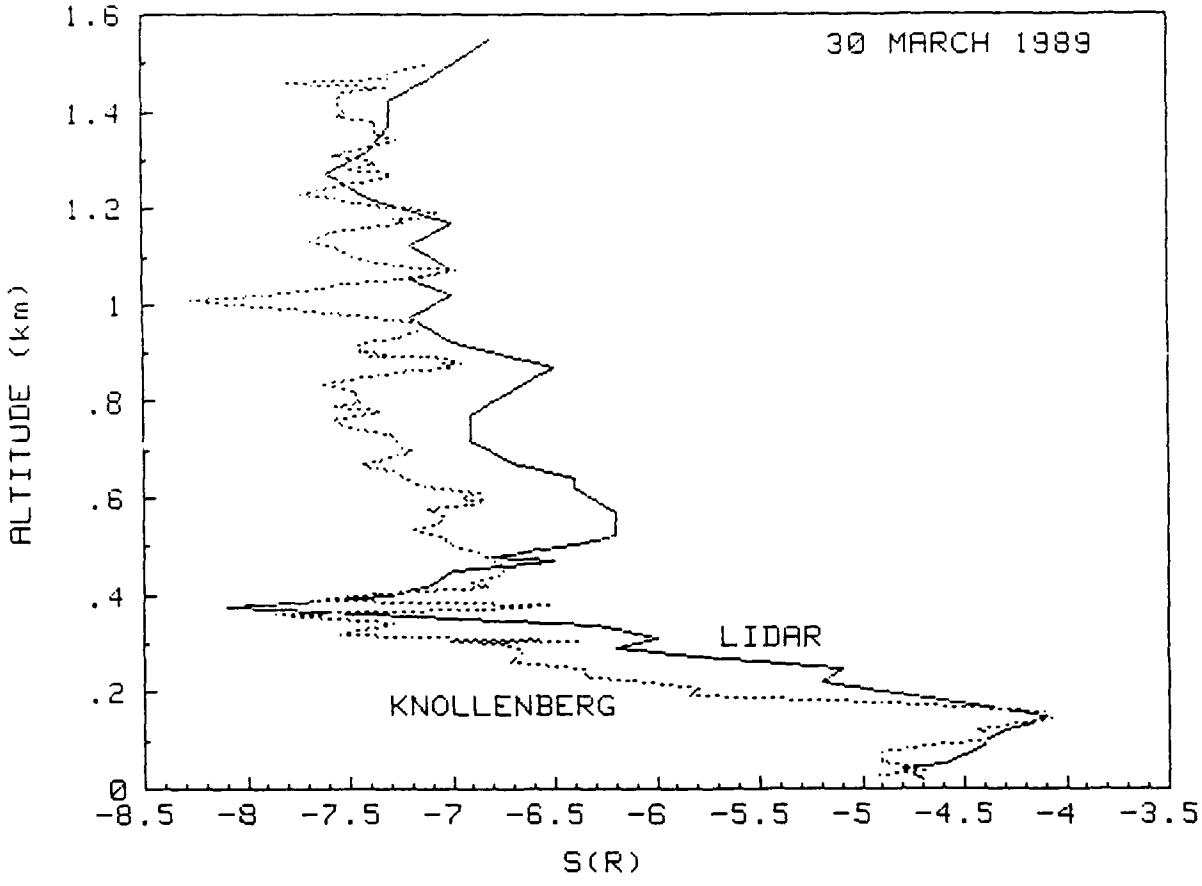

Figure 9. Comparison of lidar-measured *S(R)* as a function of altitude with that calculated with the use of Knollenberg-measured aerosol size distributions as a function of altitude.

REFERENCES

Fenn, R. W., Correlation between atmospheric backscatter and meteorological visual range, *Appl. Opt.* 5, 293 (1966).

Ferguson, J. A., and M. R. Paulson, Calibration of the hand-held lidars used by the Naval Ocean Systems Center, Naval Ocean Systems Center TD 996 (1986).

Hughes, H. G., and M. R. Paulson, Double-ended lidar technique for aerosol studies, *Appl. Opt.* 27, 2273 (1988).

Kunz, G. J., Bipath method as a way to measure the spatial backscatter and extinction coefficients with lidar, *Appl. Opt.* 26, 794 (1987).

Mulders, J. M., Algorithm for inverting lidar returns: comment, *Appl. Opt.* 23, 2855 (1984).

Paulson, M. R., Lidar measurements indicating atmospheric inhomogeneities, Naval Ocean Systems Center TD 867 (1986).

Paulson, M. R., Evaluation of a dual lidar method for measuring aerosol extinction, Naval Ocean Systems Center TD 1075 (1987).

APPENDIX

S(R) CURVES AND *S(R)* DIFFERENCE CURVES FOR DATA SETS 5 THROUGH 9

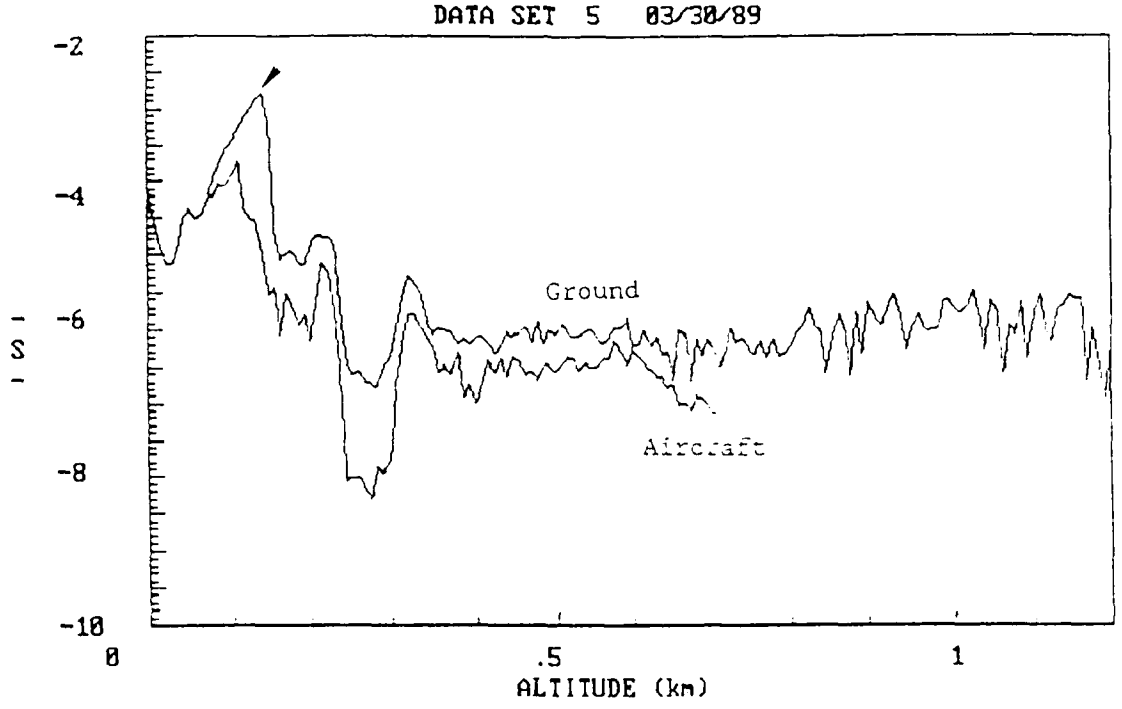

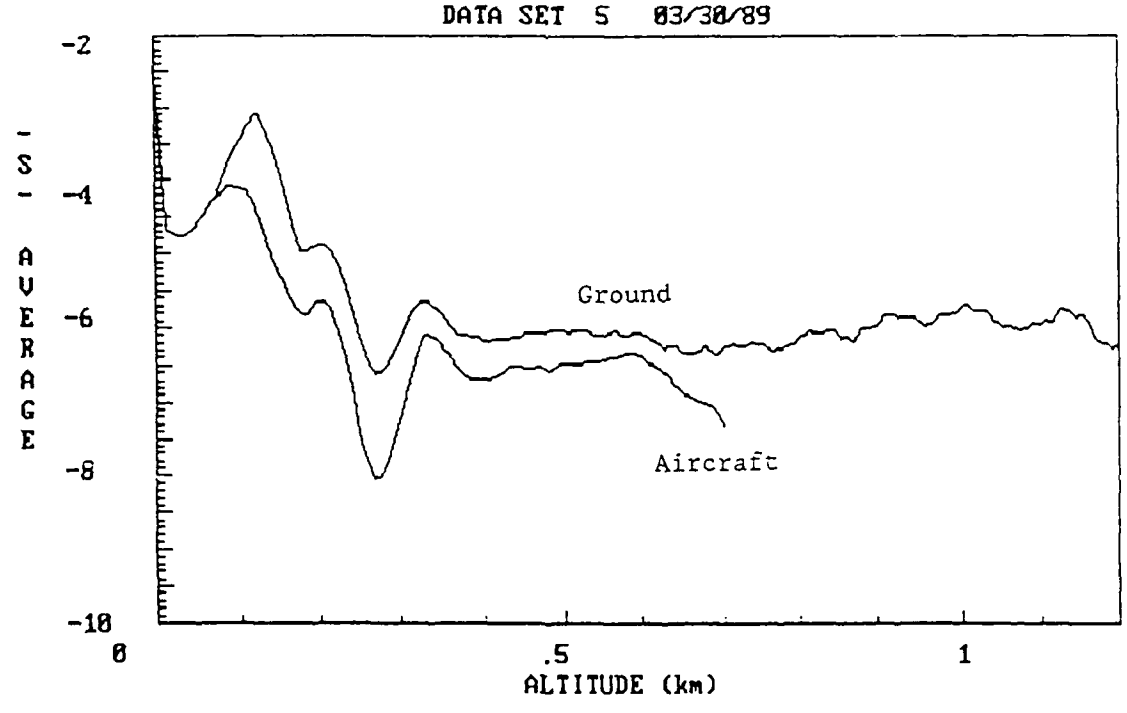

Figure A-1. *S(R)* curves for for Data Set 5. Lower curves are seven-point running averages of the upper curves.

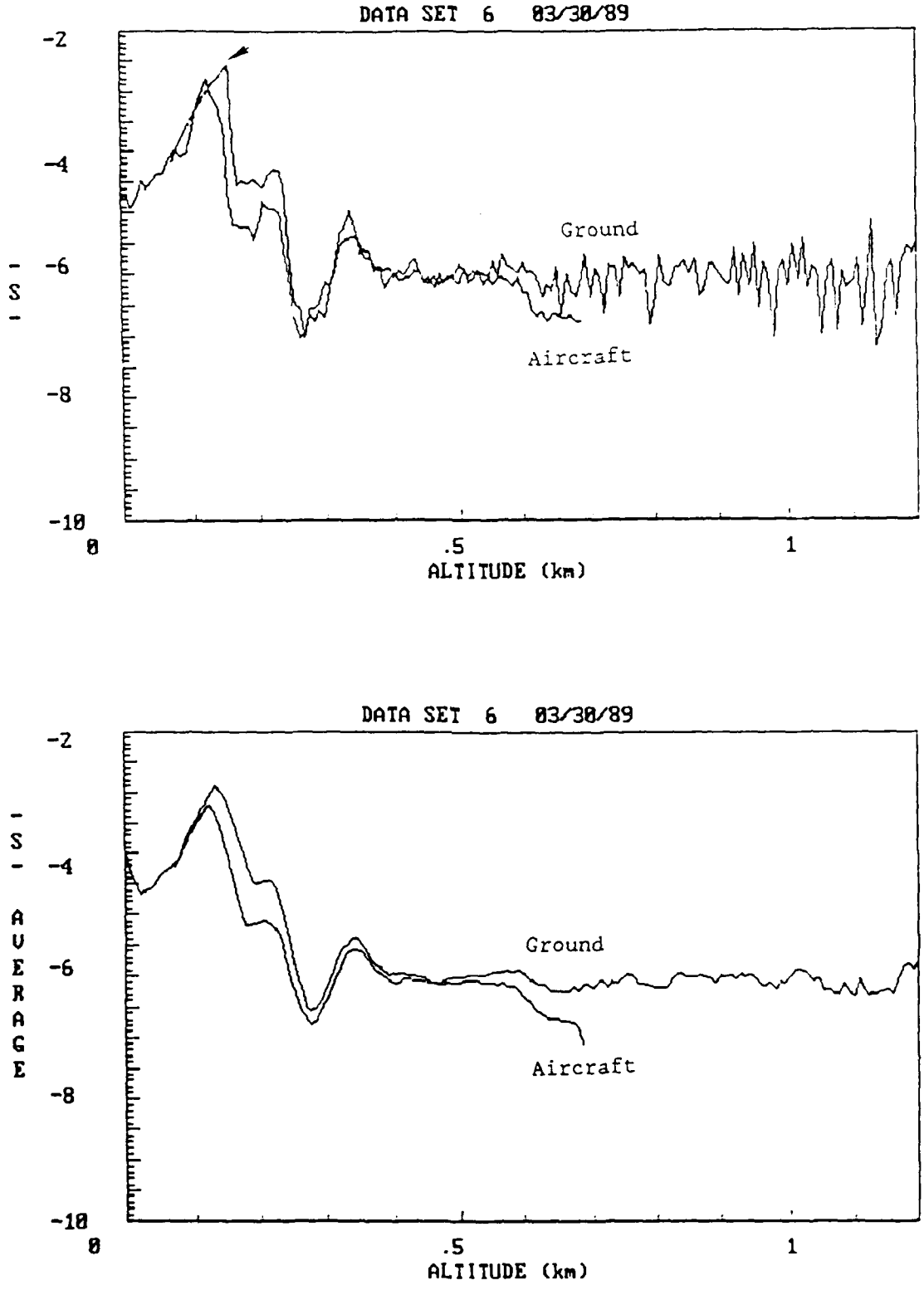

Figure A-2. *S(R)* curves for for Data Set 6. Lower curves are seven-point running averages of the upper curves.

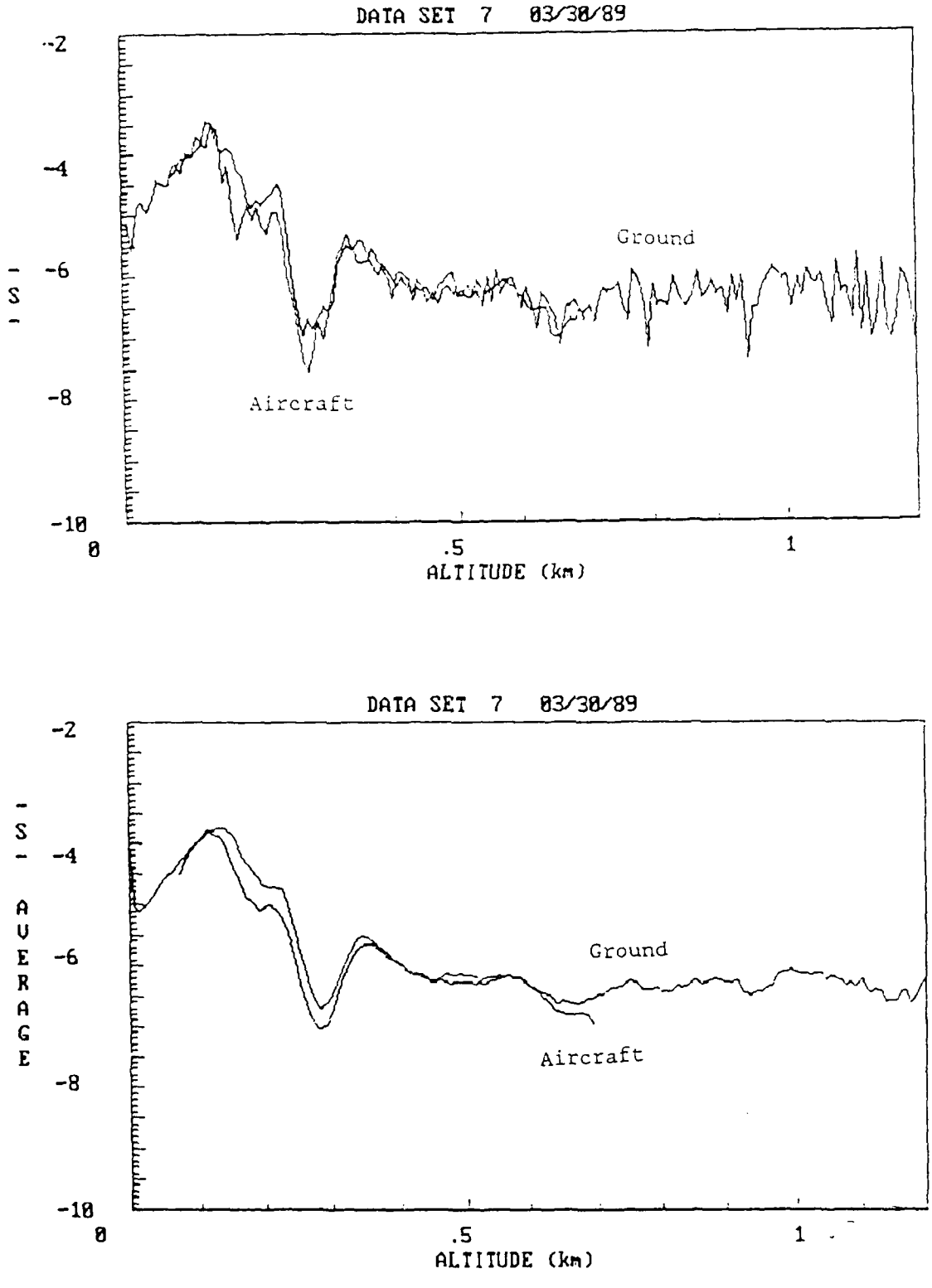

***Figure* A-3.** *S(R) curves for for* Data Set 7. Lower curves are seven-point running averages of the upper curves.

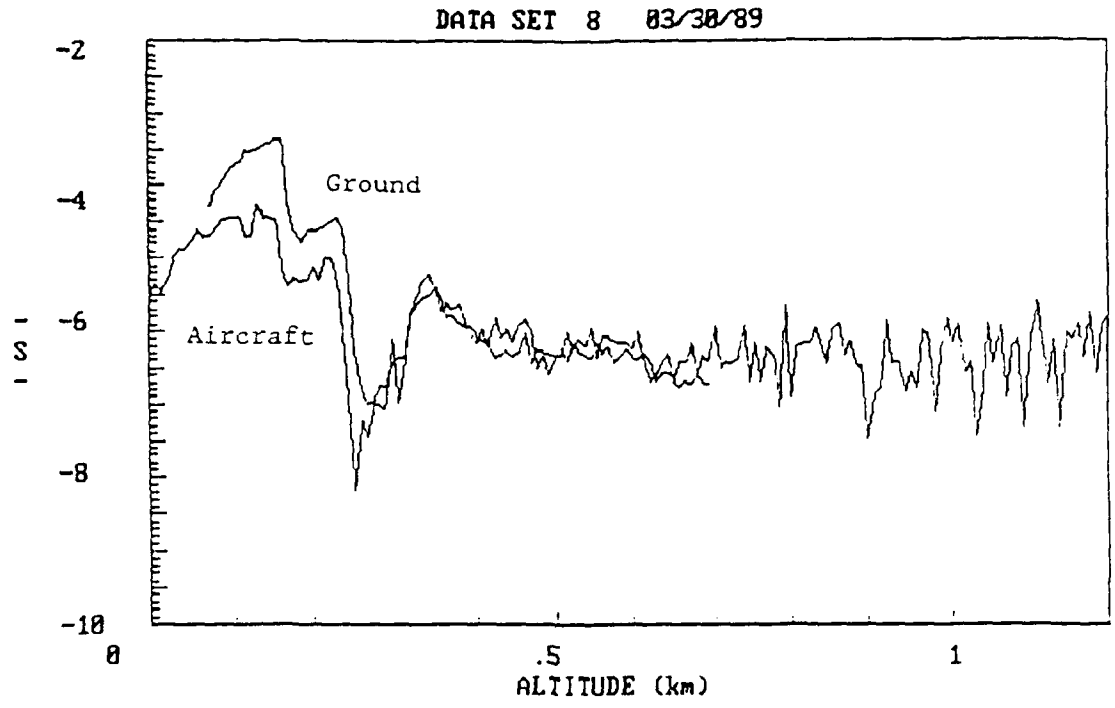

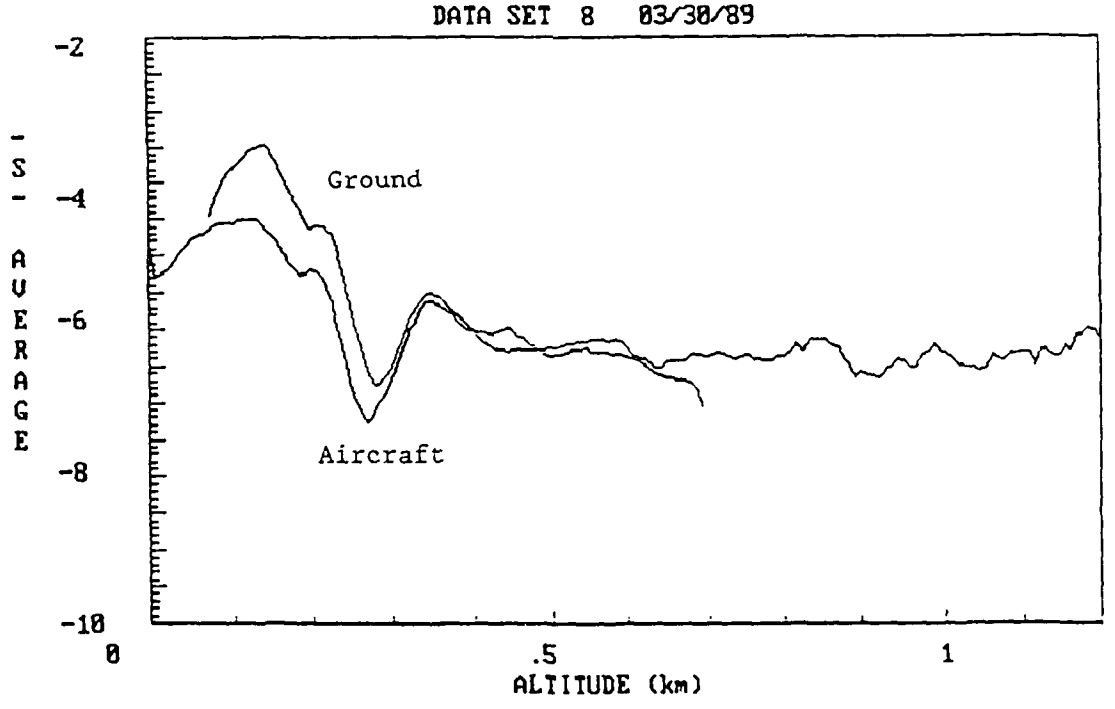

Figure A-4. *S(R)* curves for for Data Set 8. Lower curves are seven-point running averages of the upper curves.

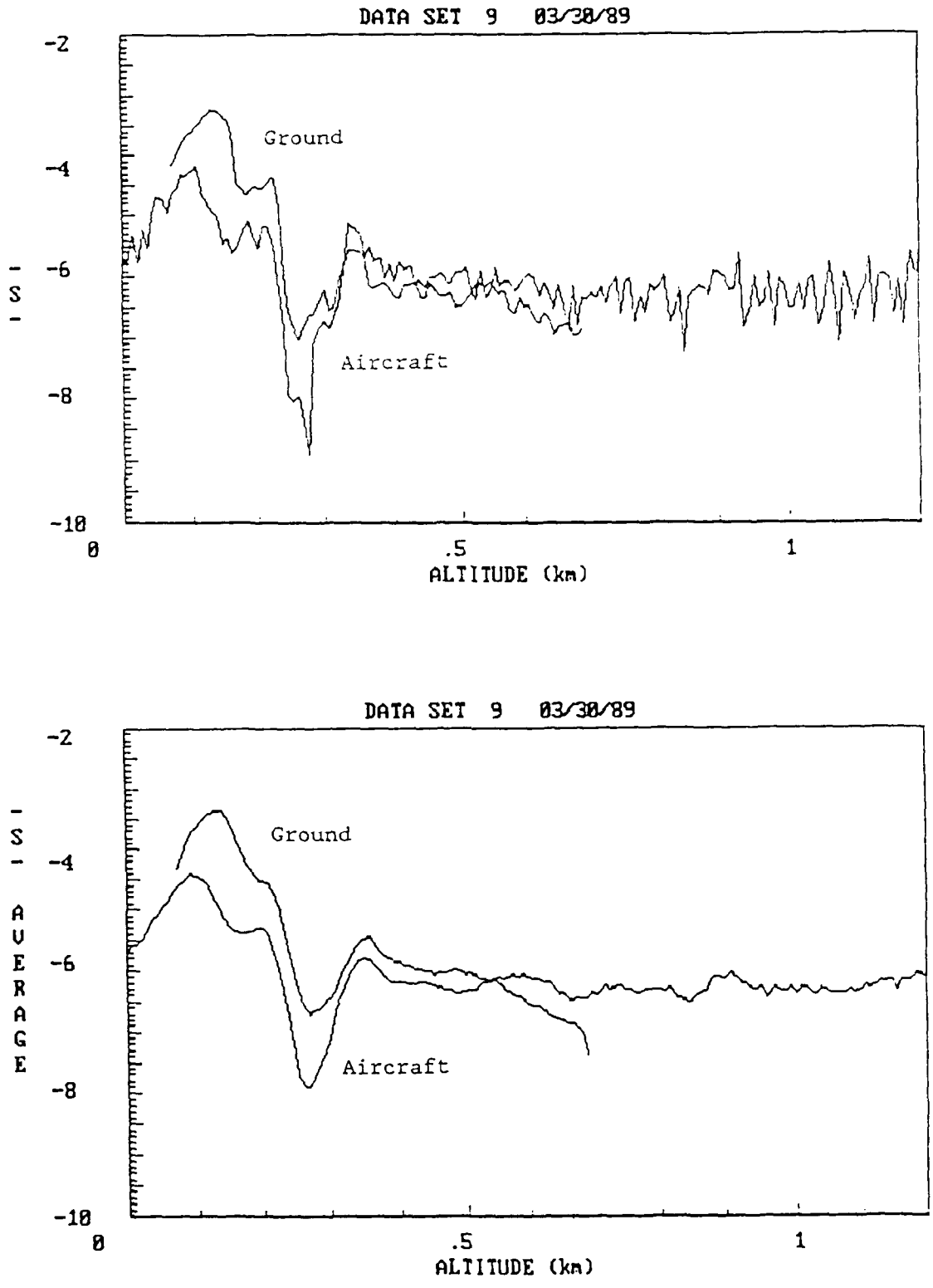

Figure A-5. *S(R)* curves for for Data Set 9. Lower curves are seven-point running averages of the upper curves.

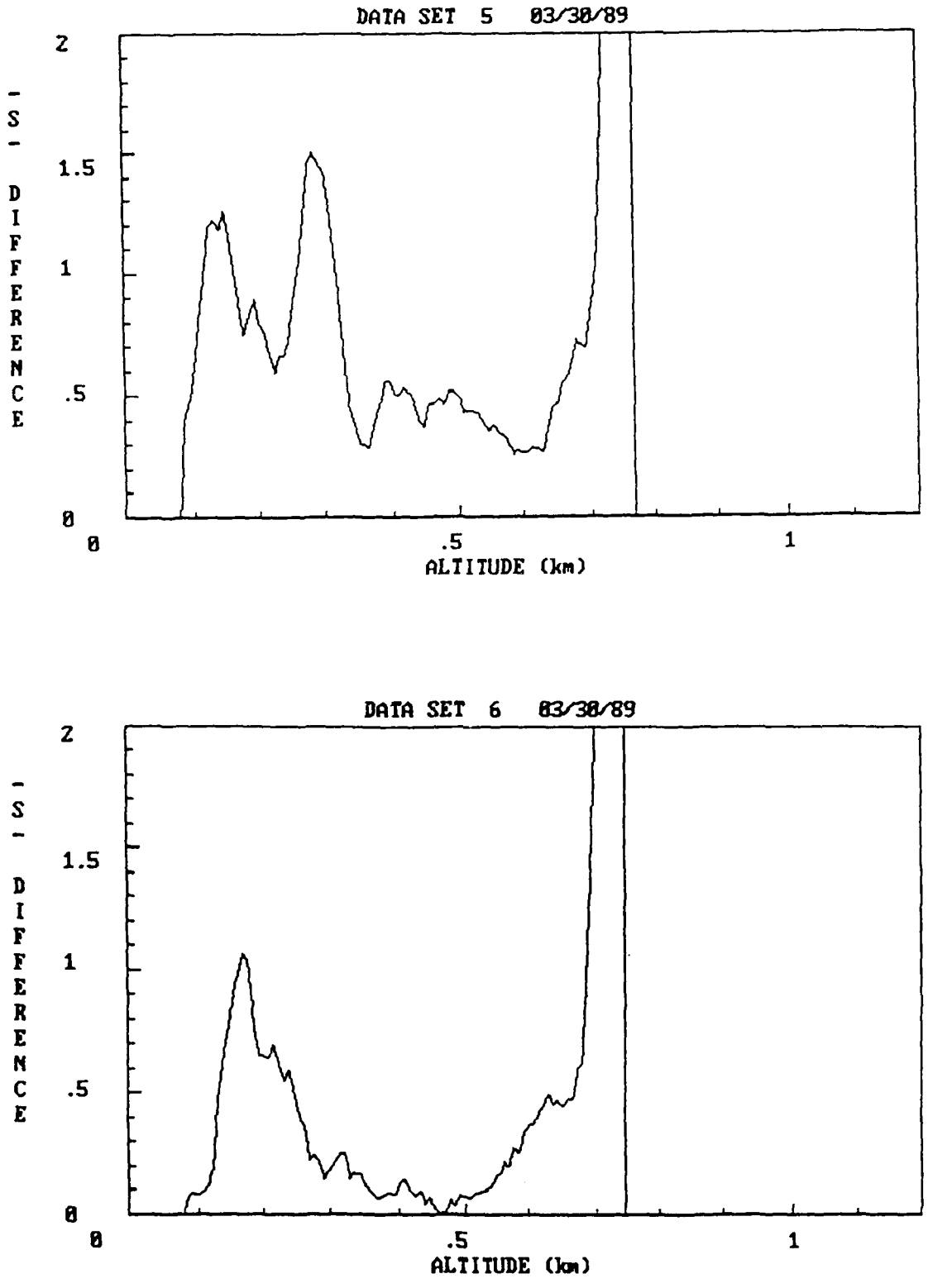

Figure A-6. Upper graph is *S(R)* difference curve for Data Set 5. Lower graph is that for Data Set 6.

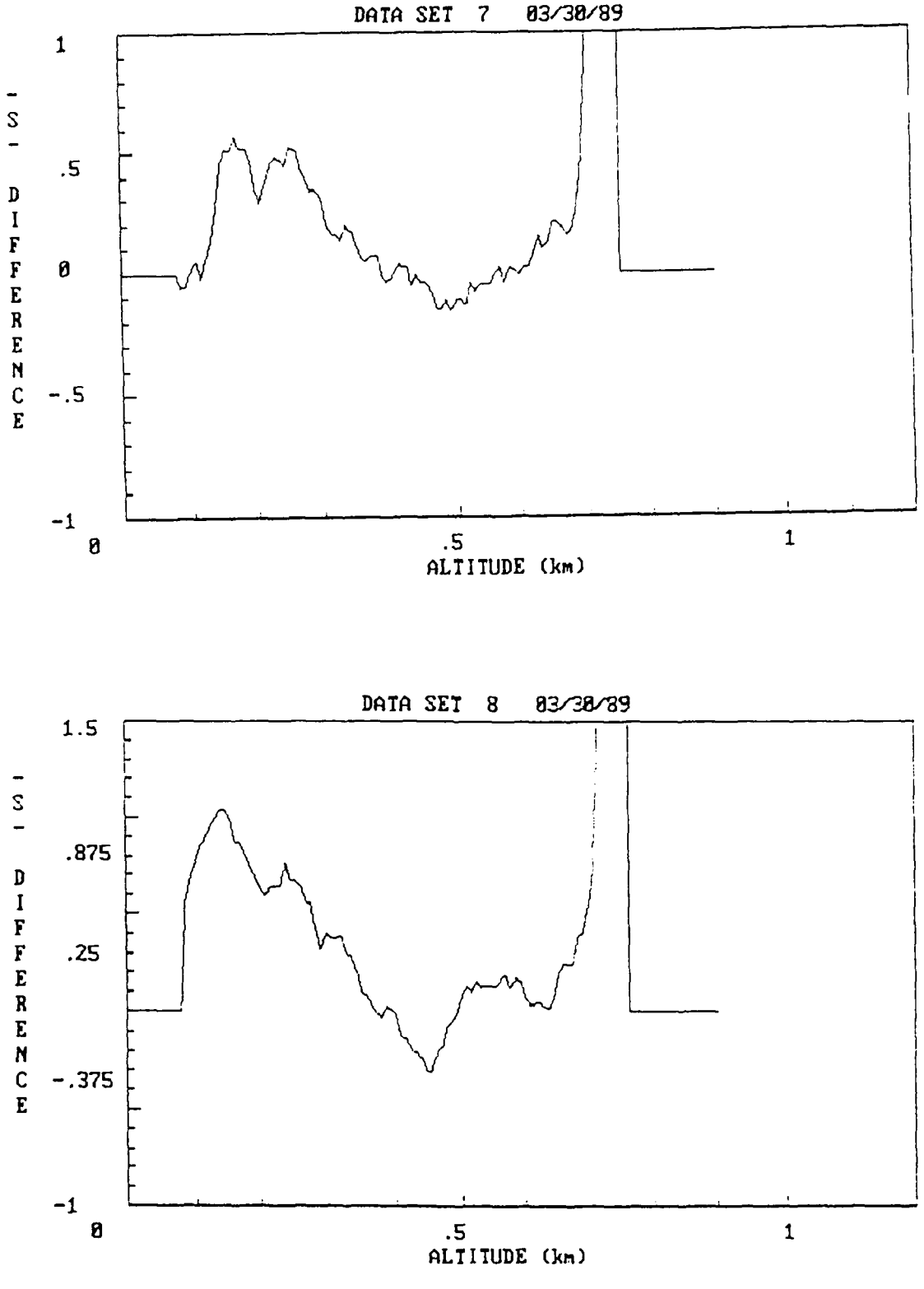

Figure A-7. Upper graph is *S(R)* difference curve for Data Set 7. Lower graph is that for Data Set 8.

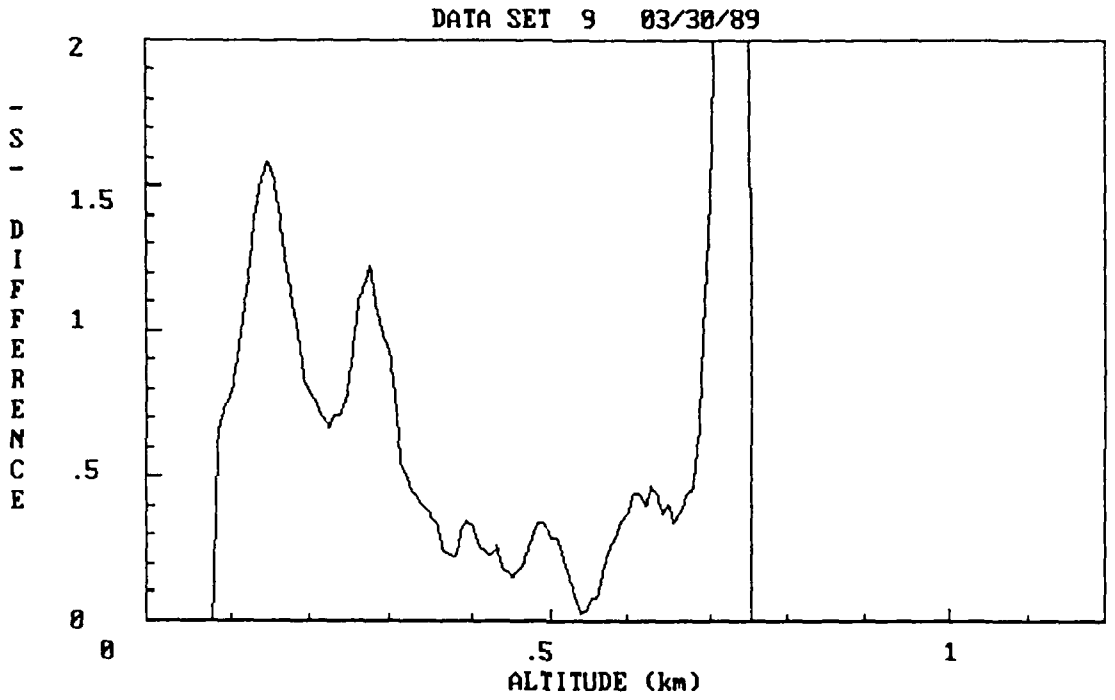

Figure A-8. *S(R)* difference curve for Data Set 9.